

Valence and spin states in delafossite AgNiO_2 and the frustrated Jahn-Teller system ANiO_2 ($A = \text{Li, Na}$)

J.-S. Kang,^{1,*} S. S. Lee,^{1,†} G. Kim,¹ H. J. Lee,¹ H. K. Song,² Y. J. Shin,² S. W. Han,³ C. Hwang,³ M. C. Jung,⁴ H. J. Shin,⁴ B. H. Kim,⁵ S. K. Kwon,⁵ and B. I. Min⁵

¹Department of Physics, The Catholic University of Korea, Bucheon 420-743, Korea

²Department of Chemistry, The Catholic University of Korea, Bucheon 420-743, Korea

³Korea Research Institute of Standards and Science, Daejeon 305-340, Korea

⁴Pohang Accelerator Laboratory (PAL), POSTECH, Pohang 790-784, Korea

⁵Department of Physics, POSTECH, Pohang 790-784, Korea

(Received 16 September 2007; published 26 November 2007)

Electronic structures of delafossite oxides $\text{AgNi}_{1-x}\text{Co}_x\text{O}_2$ and the frustrated Jahn-Teller (JT) system ANiO_2 ($A = \text{Li, Na}$) have been investigated by employing soft x-ray absorption spectroscopy and photoemission spectroscopy (PES). It is found that Ni ions are in the Ni^{2+} - Ni^{3+} mixed-valent states and that the low-spin (LS) Ni^{3+} component increases from LiNiO_2 to AgNiO_2 and NaNiO_2 , in agreement with the presence of the JT transition in NaNiO_2 and the absence of the JT transition in LiNiO_2 and AgNiO_2 . In $\text{AgNi}_{1-x}\text{Co}_x\text{O}_2$, the Ni^{3+} component increases with x , while Co ions are in the LS Co^{3+} states for all x , which is consistent with the metallic nature for low values of x . A good agreement is found between the measured PES spectra and the calculated local spin density approximation (LSDA) electronic structures of AgNiO_2 and AgCoO_2 , but the pseudogap feature in PES of AgNiO_2 is not described by the LSDA.

DOI: 10.1103/PhysRevB.76.195122

PACS number(s): 72.20.Pa, 74.25.Jb, 78.70.Dm, 79.60.-i

I. INTRODUCTION

Delafossite oxides $MM'\text{O}_2$ [$M = \text{Cu, Ag, Pd, Pt}$; $M' = \text{Al, Cr, Fe, Co, Ni, Rh, Ln}$ (lanthanides),...] have attracted renewed interest as promising candidates for p -type transparent conducting oxides¹ and also for thermoelectric materials.² M and M' ions in $MM'\text{O}_2$ are considered to be formally monovalent and trivalent, respectively.³ Most $MM'\text{O}_2$ -type delafossites crystallize in the $3R$ CuFeO_2 -type layered structure (Fig. 1) with the rhombohedral space group of $R\bar{3}m$, which is characterized by the alternating stacking of $[M'\text{O}_2]$ slabs and O- M -O dumbbell-shaped layers along the c axis.⁴ Both M and M' cations as well as O anions in each layer form triangular sublattices, and the $[M'\text{O}_2]$ slab is comprised of edge-shared $M'\text{O}_6$ octahedra. Hence, when M' ions are magnetic as in CuFeO_2 , $MM'\text{O}_2$ delafossites often exhibit the complicated antiferromagnetic (AF) ordering due to the spin frustration in the triangular lattice.⁵

Cu- and Ag-based delafossite oxides are semiconductors except for semimetallic AgNiO_2 .^{6,7} AgNiO_2 is special because it is an AF metal, while AgFeO_2 and AgCoO_2 are nonmagnetic insulators. A compositionally controlled metal-insulator (M - I) transition has been observed⁸ in $\text{AgNi}_{1-x}\text{Co}_x\text{O}_2$ with increasing x . Magnetic susceptibility measurements suggest the low-spin (LS) Ni^{3+} ($t_{2g}^3 t_{2g}^3 e_g^1$) and LS Co^{3+} ($t_{2g}^3 t_{2g}^3 e_g^1$) states, respectively.⁸ Hence, AgNiO_2 has been studied as a good model system of the geometrically frustrated magnet with $S = 1/2$ Ni^{3+} ions. On the other hand, our previous work⁹ for AgTO_2 ($T = \text{Fe, Co, Ni}$) showed that Fe and Co ions are trivalent, but that Ni ions are in the Ni^{2+} - Ni^{3+} mixed-valent states with significantly large divalent character. The finding of Fe^{3+} and Co^{3+} ions agrees with magnetic susceptibility data, but the existence of Ni^{2+} ions seems to be contradictory to the magnetic susceptibility data.⁸

The existence of Ni^{2+} states in AgNiO_2 has been questioned recently in relation to the issue of the subvalent Ag ions in Ag_2NiO_2 .¹⁰ Note that there is a similar controversy on the valence states of Ni ions in LiNiO_2 that is a prototype anode material for Li-ion batteries.¹¹⁻¹³ LiNiO_2 has the α - NaFeO_2 -type layered structure that is very similar to the CuFeO_2 type of AgNiO_2 (Fig. 1). As in AgNiO_2 , LiNiO_2 does not exhibit a Jahn-Teller (JT)-induced orbital ordering^{7,14} in contrast to its sister compound NaNiO_2 that has both the spin ordering and the JT-induced orbital orderings.¹⁵ NaNiO_2 transforms from a rhombohedral to a monoclinic structure below ~ 480 K. The origin of the absence and the presence of the orderings in ANiO_2 ($A = \text{Li, Na}$) is one of the hot subjects in the frustrated JT systems with the 90° superexchange.¹⁴ Therefore, the systematic investigation of the valence and spin states of Co and Ni ions in $\text{AgNi}_{1-x}\text{Co}_x\text{O}_2$ and ANiO_2 ($A = \text{Li, Na}$) is crucial in

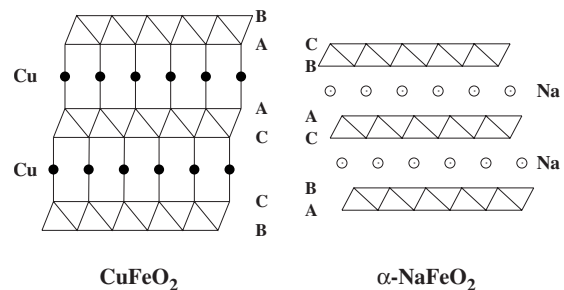


FIG. 1. Comparison of the $3R$ -delafossite CuFeO_2 structure and α - NaFeO_2 structure. Both have $R\bar{3}m$ space group. The layers of edge-shared FeO_6 octahedra are separated by Cu or Na layers. Cu and Na ions are located at the O-Cu-O dumbbell centers and the NaO_6 octahedral centers, respectively. A, B, and C represent the stacking order of oxide layers.

understanding the M - I transition in $\text{AgNi}_{1-x}\text{Co}_x\text{O}_2$ and the origin of the spin and orbital orderings in ANiO_2 .

Soft x-ray absorption spectroscopy (XAS) is an important experimental tool for studying the valence and spin states of T ions in solids.^{16–18} Photoemission spectroscopy (PES) is ideal for studying the electronic structures of solids, such as the energy distribution of different electronic orbitals.^{19,20} In this work, we have investigated the electronic structures of $\text{AgNi}_{1-x}\text{Co}_x\text{O}_2$ ($0 \leq x \leq 1$) using PES and XAS. We have determined the valence states and spin configurations of Ni and Co ions in $\text{AgNi}_{1-x}\text{Co}_x\text{O}_2$ and addressed the issue of the valence states of Ni ions in ANiO_2 ($A=\text{Li}, \text{Na}$). We have compared the valence-band PES and O $1s$ XAS spectra with the calculated electronic structures and determined the character of the carriers near the Fermi level (E_F) in $\text{AgNi}_{1-x}\text{Co}_x\text{O}_2$.

II. EXPERIMENTAL DETAILS

Polycrystalline $\text{AgNi}_{1-x}\text{Co}_x\text{O}_2$ samples were prepared by cation-exchange reaction methods, as described in Ref. 8. PES and XAS experiments were performed at the 8A1 undulator beamline of the Pohang Accelerator Laboratory (PAL) at room temperature (RT). The base pressure was better than 3×10^{-10} Torr. Samples were cleaned *in situ* by repeated scraping with a diamond file. The data presented in this paper were reproduced several times, which confirms that they are free of surface contamination. XAS spectra were obtained by employing the total electron yield mode with the photon energy resolution of ~ 100 meV at $h\nu \sim 700$ eV. The Fermi level E_F and the instrumental resolution of the system were determined from the valence-band spectrum of scraped Pd in electrical contact with samples. The instrumental resolution for the valence-band PES spectra was set at ~ 200 meV at $h\nu \sim 200$ eV. All the XAS and PES spectra were normalized to the incident photon flux.

III. RESULTS AND DISCUSSION

Figure 2(a) shows the measured Co $2p$ XAS spectra of $\text{AgNi}_{1-x}\text{Co}_x\text{O}_2$. As a guide of the valence states of Co ions, these data are compared to those of reference Co oxides, such as CoO (Ref. 21) as a formally high-spin Co^{2+} oxide ($3d^7$), LiCoO_2 (Ref. 11) as a formally LS Co^{3+} oxide ($3d^6$), $\text{Na}_{0.5}\text{CoO}_2$ (Ref. 22) as a formally mixed-valent $\text{Co}^{3+}(3d^6)$ - $\text{Co}^{4+}(3d^5)$ oxide, and that of Co metal.²³ At the bottom, the calculated XAS spectrum for a LS Co^{3+} ion ($d^6: t_{2g}^3 e_g^3$) is shown by employing the ligand-field multiplet (LFM) model^{16,17} with the crystal field splitting energy of $10Dq=3.0$ eV between t_{2g} and e_g states. This comparison shows that (i) the Co $2p$ XAS spectra of $\text{AgNi}_{1-x}\text{Co}_x\text{O}_2$ are very similar to each other, (ii) they are nearly identical to that of LiCoO_2 , and (iii) they are described well by the LFM model calculation for a LS Co^{3+} ion.

These findings suggest that Co ions in $\text{AgNi}_{1-x}\text{Co}_x\text{O}_2$ are in the LS trivalent Co^{3+} states and that the valence states of Co ions do not change with varying x . Also notable is that, except for the low-energy shoulder at $h\nu \approx 781$ eV, the Co $2p$ XAS spectrum of AgCoO_2 is similar to that of

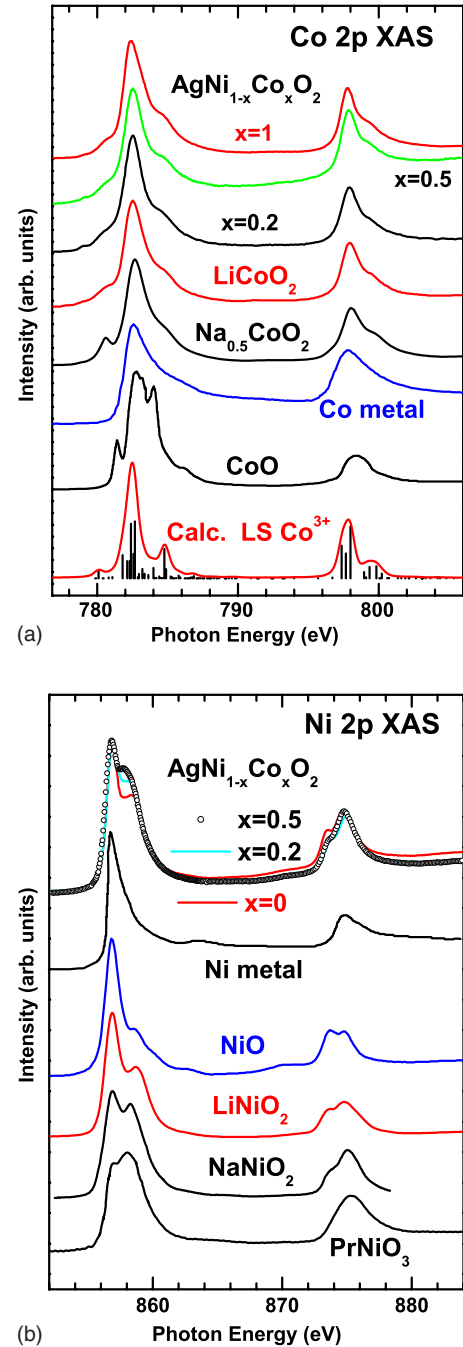


FIG. 2. (Color online) (a) Co $2p$ XAS spectra of $\text{AgNi}_{1-x}\text{Co}_x\text{O}_2$ compared to those of LiCoO_2 , $\text{Na}_{0.5}\text{CoO}_2$, CoO, Co metal, and the calculated XAS for a LS Co^{3+} ion. (b) Ni $2p$ XAS spectra of $\text{AgNi}_{1-x}\text{Co}_x\text{O}_2$ compared to those of Ni metal, NiO, LiNiO_2 , NaNiO_2 , and PrNiO_3 .

$\text{Na}_{0.5}\text{CoO}_2$, which has a good thermoelectric property²⁴ as well as a superconducting property with water intercalation.²⁵ This shoulder ($h\nu \approx 781$ eV) reflects the Co^{4+} contribution coming from the Na deficiency.²⁶ Therefore, in view of similar crystal structures between AgCoO_2 and NaCoO_2 , Ag-deficient Ag_xCoO_2 will be a promising system for exploiting such features as realized in Na_xCoO_2 .

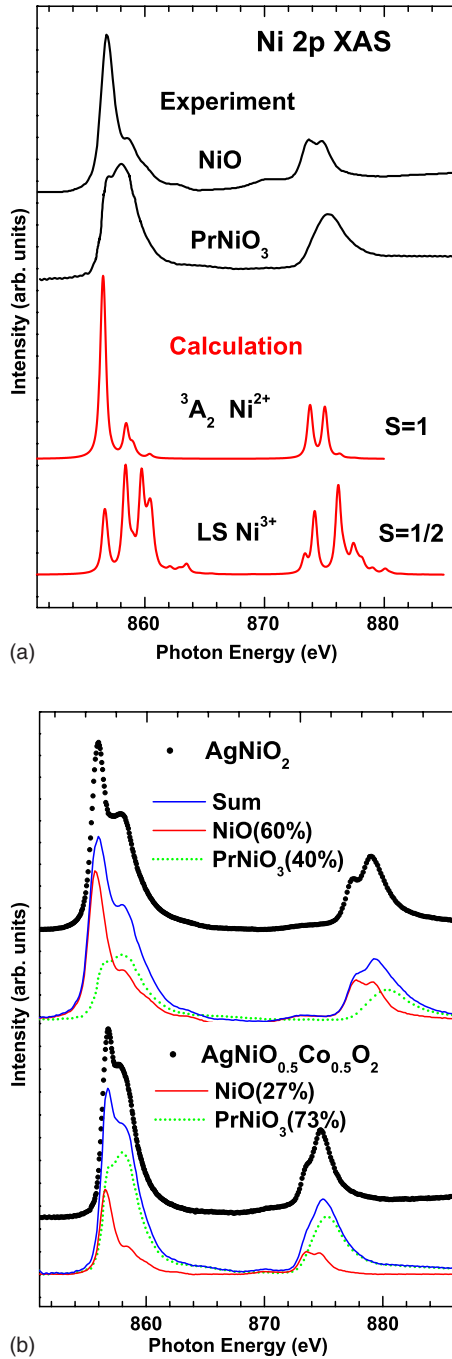


FIG. 3. (Color online) (a) Comparison of the measured XAS spectra of NiO and PrNiO₃ with the calculated Ni 2p XAS spectra for ³A₂ Ni²⁺ and LS Ni³⁺ ions. (b) Comparison of the Ni 2p XAS spectra of AgNiO₂ and AgNi_{0.5}Co_{0.5}O₂ to the weighted sum of those of NiO and PrNiO₃.

Similarly, Fig. 2(b) compares the Ni 2p XAS spectra of AgNi_{1-x}Co_xO₂ to those of NiO (Ref. 11) as a formally divalent Ni²⁺ oxide (3d⁸), PrNiO₃ (Ref. 27) as a formally trivalent Ni³⁺ oxide (3d⁷),²⁸ and that of Ni metal (Ref. 21). LiNiO₂ (Ref. 11) and NaNiO₂ (Ref. 29) are also included since both have locally the same NiO₆ environment as AgNiO₂. This comparison shows that the line shapes of the Ni 2p XAS spectra of AgNi_{1-x}Co_xO₂ are in between those of

NiO and PrNiO₃ (see Fig. 3), and the intensity of the high-energy shoulder ($h\nu \approx 859$ eV) increases with increasing x .

Figure 3(a) compares the measured Ni 2p XAS spectra of NiO and PrNiO₃ with the calculated Ni 2p XAS spectra for ³A₂ Ni²⁺ ($t_{2g}^3 e_g^2 t_{2g}^3$) and LS Ni³⁺ (${}^2E: t_{2g}^3 e_g^1 t_{2g}^3 e_g^1$), with $10Dq = 2.4$ eV for Ni²⁺ and $10Dq = 3.0$ eV for LS Ni³⁺. These LFM model calculations reveal that the qualitative features of the Ni 2p XAS spectra of NiO and PrNiO₃ can be described by ³A₂ Ni²⁺ and LS Ni³⁺ configurations, respectively. In the quantitative aspect, however, the LFM calculations do not yield very good agreement with experiment. Hence, for the analysis of the valence states, we present the comparison of the measured Ni 2p XAS spectra of AgNi_{1-x}Co_xO₂ to the weighted sum of those of NiO and PrNiO₃. As shown in Fig. 3(b), a good agreement is obtained, and the observed trend with x is reproduced well by increasing the weight of Ni³⁺ (PrNiO₃) with respect to that of Ni²⁺ (NiO). That is, the ratio of Ni²⁺:Ni³⁺ varies from 60%:40% for $x=0$ to 27%:73% for $x=0.5$. This finding confirms that Ni ions in AgNi_{1-x}Co_xO₂ are in the Ni²⁺-Ni³⁺ mixed-valent states and that the Ni³⁺ component increases with x .

Semiconducting AgCoO₂ reveals only trivalent Co³⁺ ions, whereas semimetallic AgNiO₂ reveals mixed-valent Ni ions. This suggests that the mixed-valent Ni ions play a crucial role in determining the metallic ground states of AgNi_{1-x}Co_xO₂ for low x values and the $M-I$ transition with increasing x . It is likely that Ni²⁺ ions induce hole carriers in the O 2p-Ni 3d hybridized bands of AgNi_{1-x}Co_xO₂, so as to make the system metallic.

The existence of Ni²⁺ ions in AgNiO₂ is not unexpected. In contrast to Co³⁺ in the LS state, Ni³⁺ in the LS state, which has the half-filled e_g orbital, would not be stable energetically in an octahedral (O_h) environment. That is, without the JT distortion, the Ni²⁺ state would be more stable than the LS Ni³⁺ state. Our finding on the existence of the Ni²⁺ states in AgNiO₂ is contradictory to that of Ref. 10, where it was concluded that Ni ions are trivalent in AgNiO₂ based on the Ni K -edge (1s) XAS. We think that the Ni L -edge (2p) XAS provides a more direct information on the occupied configuration of the 3d electrons than the Ni K -edge XAS because the Ni L edge is determined by the $2p \rightarrow 3d$ absorption while the K edge is determined by the $1s \rightarrow 4p$ absorption. Therefore, our conclusion drawn from the Ni 2p XAS will be more reliable than that of Ref. 10.

Recently, the neutron diffraction experiment for 2H-type AgNiO₂ has been reported.³⁰ They analyzed the data by invoking the charge ordering (CO) with three nonequivalent Ni sites, with one Ni²⁺ site and two metallic Ni^{3.5+} sites. Our finding on the Ni²⁺-Ni³⁺ mixed-valent states in AgNiO₂ seems to be contradictory to this interpretation for 2H-type AgNiO₂.³⁰ However, since our XAS data for AgNi_{1-x}Co_xO₂ were obtained at RT, we think that it is not necessary to take into account the CO in the interpretation of our XAS data. Further, the XAS study on transition-metal oxides is supposed to provide more direct information on the valence states of transition-metal ions than the bond length argument employed in the analysis of neutron diffraction.³⁰

The high-energy shoulder at $h\nu \approx 859$ eV increases from NiO to LiNiO₂, AgNiO₂, AgNi_{0.5}Co_{0.5}O₂, and NaNiO₂ [see

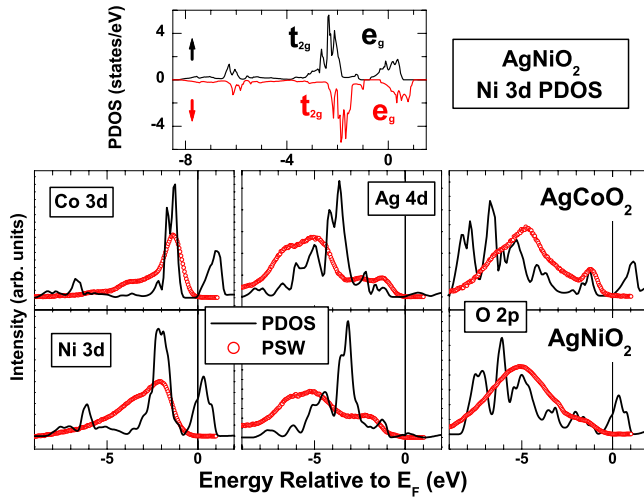


FIG. 4. (Color online) (Top) Calculated Ni 3d PDOS for AgNiO₂. (Middle) Comparison of the Co 3d, Ag 4d, and O 2p PSW's with the corresponding calculated PDOS's for AgCoO₂. (Bottom) Similarly for AgNiO₂.

Fig. 2(b)]. The ratio of this shoulder to the main peak is given by ~ 0.33 (NiO), ~ 0.56 (LiNiO₂), ~ 0.62 (AgNiO₂), ~ 0.81 (AgNi_{0.5}Co_{0.5}O₂), and ~ 0.86 (NaNiO₂), suggesting the increasing Ni³⁺ component. Since Ni³⁺ ions in the LS state are JT active in the O_h environment, as explained above, the trend of the increasing Ni³⁺ component is consistent with the presence of the JT structural transition in NaNiO₂ and the absence of the JT transition in NiO and LiNiO₂. In the same context, the absence of the cooperative JT transition in AgNiO₂ can be understood by its Ni²⁺-Ni³⁺ mixed-valent nature. We think that the present finding resolves the controversial issue on the valence states of Ni ions in AgNiO₂ and ANiO₂ (A=Li, Na).

Figure 4 compares the experimental partial spectral weight (PSW) distributions of the different electronic states with the calculated partial density of states (PDOS) of the corresponding states. The experimental Ag 4d, Co/Ni 3d, and O 2p PSW's were determined from the measured valence-band PES spectra over a wide photon energy range ($30 \text{ eV} \leq h\nu \leq 1486.6 \text{ eV}$) by employing the extraction procedures described in Refs. 9 and 20. The calculated PDOS's were obtained by using the self-consistent linearized muffin-tin orbital band method within the local spin density approximation (LSDA), where the paramagnetic and ferromagnetic ground states were assumed for AgCoO₂ and AgNiO₂, respectively.³¹ The calculated PDOS's are similar to those in literature.³ The LSDA calculation gives a better agreement with experiment than the LSDA+*U* calculation ($U=5 \text{ eV}$), with *U* being the Coulomb correlation between Ni 3d electrons.

LSDA band calculations produce the correct semiconducting and LS ground state for AgCoO₂ and the metallic and magnetic ground states for AgNiO₂. Co 3d bands show a gap between the occupied t_{2g} states and the unoccupied e_g states. The small magnetic moment M_s of $\sim 0.5 \mu_B$ per Ni for AgNiO₂ is in good agreement with the magnetic susceptibility measurement.⁸ The calculated Ag 4d bands are fully oc-

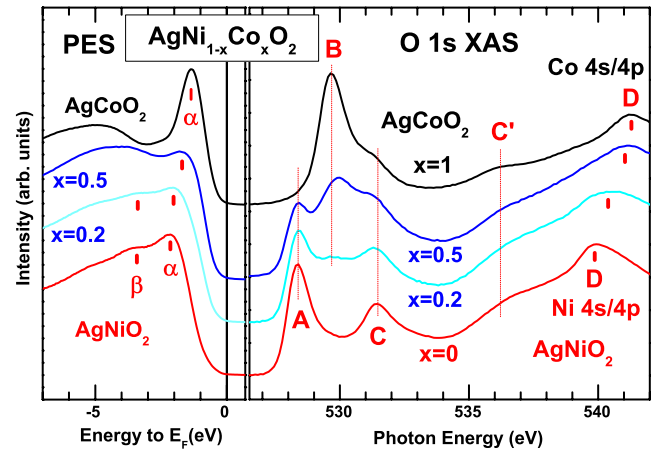


FIG. 5. (Color online) (Left) Comparison of the valence-band PES spectra of AgNi_{1-x}Co_xO₂ obtained with $h\nu=130 \text{ eV}$. (Right) O 1s XAS spectra of AgNi_{1-x}Co_xO₂. Each feature is identified as follows: α in AgCoO₂: the occupied Co $t_{2g} \uparrow \downarrow$ states; α and β in AgNiO₂: the occupied minority Ni $t_{2g} \downarrow$ and majority Ni $t_{2g} \uparrow$ states; A: the unoccupied Ni $e_g \uparrow \downarrow$ states; B: the unoccupied Co $e_g \uparrow \downarrow$ states; C, C': the unoccupied Ag *sp* states; and D: the unoccupied Ni/Co *sp* states.

cupied, indicating monovalent Ag⁺ states. Figure 4 reveals a reasonably good agreement between experiment and theory. In particular, the peak positions of both the Co 3d and Ni 3d states agree well between experiment and theory. The trends observed in PES are consistent with those in the calculated PDOS. The occupied bandwidth of the Ni 3d states is broader than that of the Co 3d states, which supports the large hybridization between Ni 3d and O 2p states.

Figure 5 compares the $h\nu=130 \text{ eV}$ valence-band PES spectra (left) and the O 1s XAS spectra (right) of AgNi_{1-x}Co_xO₂. The $h\nu=130 \text{ eV}$ PES spectra are chosen as roughly representing the main features of the Co/Ni 3d PSW's.⁹ The O 1s XAS spectrum is attributed to the unoccupied *T* 3d, Ag *sp*, and *T* *sp* states ($T=\text{Co, Ni}$) via the hybridization with the O 2p states. The peak α in PES of AgCoO₂ represents the occupied Co t_{2g} paramagnetic states. The peaks α and β in PES of AgNiO₂ represent the occupied minority Ni $t_{2g} \downarrow$ and majority Ni $t_{2g} \uparrow$ states, respectively, and the so splitting between α and β is a rough measure of the exchange splitting $\Delta_x \sim 1.5 \text{ eV}$. This value is larger than the calculated $\Delta_x \sim 0.7 \text{ eV}$ in the LSDA (see Fig. 4). Peaks A and B in the O 1s XAS represent the unoccupied $e_g \uparrow \downarrow$ states of Ni and Co ions, respectively. Peaks C and C' are assigned as the unoccupied Ag *sp* states and D as the unoccupied Ni/Co *sp* states.

Note that the spectral weight near E_F is negligible in the valence-band PES spectra for all *x*. This feature is consistent with the semiconducting nature of AgCoO₂, but it is contradictory to the metallic nature of AgNiO₂, where $e_g \uparrow \downarrow$ states are expected to be partially occupied. This discrepancy is probably related to the high residual resistivity of AgNiO₂ ($\rho \geq 5 \text{ m}\Omega \text{ cm}$),^{6,7} a typical value of a bad metal. In bad metals, the spectral weight near E_F is occasionally suppressed by exhibiting a pseudogap feature. Even though several mechanisms are possible for the pseudogap formation in bad met-

als, the specific origin in AgNiO_2 needs to be clarified. In order to observe the metallic Fermi edge, high-resolution PES on single-crystalline samples will be required.

IV. CONCLUSIONS

In conclusion, the $2p$ XAS spectra for $\text{AgNi}_{1-x}\text{Co}_x\text{O}_2$ ($0 \leq x \leq 1$) provide evidence that Ni ions are in the Ni^{2+} - Ni^{3+} mixed-valent states with the increasing Ni^{3+} components with x , while Co ions are in the LS Co^{3+} states for all x . The metallic nature for low values of x in $\text{AgNi}_{1-x}\text{Co}_x\text{O}_2$ arises from the hole carriers in the O $2p$ -Ni $3d$ hybridized bands due to the existence of divalent Ni^{2+} ions. The LS Ni^{3+} component increases from NiO to LiNiO_2 , AgNiO_2 , $\text{AgNi}_{0.5}\text{Co}_{0.5}\text{O}_2$, and NaNiO_2 , which is consistent with the

presence of the JT structural transition in NaNiO_2 and the absence of that in LiNiO_2 and AgNiO_2 . This finding settles down the controversy on the valence states of Ni ions in AgNiO_2 and ANiO_2 ($A=\text{Li, Na}$). A good agreement is found between the measured PES spectra and the calculated LSDA electronic structures of AgNiO_2 and AgCoO_2 . The pseudogap feature near E_F in PES of AgNiO_2 , contrary to its metallic nature, remains to be resolved.

ACKNOWLEDGMENTS

This work was supported by KRF (KRF-2006-311-C00277), KOSEF through CSCMR at SNU and eSSC at POSTECH, and the basic research program of KOSEF (R01-2006-000-10369-0). PAL is supported by the MOST and POSCO in Korea.

*kangjs@catholic.ac.kr

[†]Present address: KRISS, Daejeon 305-340, Korea.

¹H. Kawazoe, M. Yasukawa, H. Hyodo, M. Kurita, H. Yanagi, and H. Hosono, *Nature (London)* **389**, 939 (1997).

²T. Okuda, N. Jufuku, S. Hidaka, and N. Terada, *Phys. Rev. B* **72**, 144403 (2005).

³R. Seshadri, C. Felser, K. Thieme, and W. Tremel, *Chem. Mater.* **10**, 2189 (1998).

⁴Y. J. Shin, J. H. Kwak, and S. Yoon, *Bull. Korean Chem. Soc.* **18**, 775 (1997).

⁵W. M. Xu, M. P. Pasternak, and R. D. Taylor, *Phys. Rev. B* **69**, 052401 (2004).

⁶A. Wichainchai, P. Dordor, J. P. Doumerc, E. Marquestaut, M. Pouchard, and P. Hagenmuller, *J. Solid State Chem.* **74**, 126 (1988).

⁷Y. J. Shin, J. P. Doumerc, P. Dordor, C. Delmas, M. Pouchard, and P. Hagenmuller, *J. Solid State Chem.* **107**, 303 (1993).

⁸Y. J. Shin, J. P. Doumerc, P. Dordor, M. Pouchard, and P. Hagenmuller, *J. Solid State Chem.* **107**, 194 (1993).

⁹S. S. Lee, J. H. Kim, S. C. Wi, G. Kim, J.-S. Kang, Y. J. Shin, S. W. Han, K. H. Kim, H. J. Song, and H. J. Shin, *J. Appl. Phys.* **97**, 10A309 (2005).

¹⁰U. Wedig, P. Adler, J. Nuss, H. Modrow, and M. Jansen, *Solid State Sci.* **8**, 753 (2006).

¹¹L. A. Montoro, M. Abbate, E. C. Almeida, and J. M. Rosolen, *Chem. Phys. Lett.* **309**, 14 (1999).

¹²Y. Uchimoto, H. Sawada, and T. Yao, *J. Power Sources* **97-98**, 326 (2001).

¹³Y. Koyama, T. Mizoguchi, H. Ikeno, and I. Tanaka, *J. Phys. Chem. B* **109**, 10749 (2005).

¹⁴M. V. Mostovoy and D. I. Khomskii, *Phys. Rev. Lett.* **89**, 227203 (2002).

¹⁵E. Chappel, M. D. Nunez-Regueiro, G. Chouteau, O. Isnard, and C. Darie, *Eur. Phys. J. B* **17**, 615 (2000).

¹⁶F. M. F. de Groot, J. C. Fuggle, B. T. Thole, and G. A. Sawatzky, *Phys. Rev. B* **42**, 5459 (1990).

¹⁷G. van der Laan and I. W. Kirkman, *J. Phys.: Condens. Matter* **4**,

4189 (1992).

¹⁸S. C. Wi, J.-S. Kang, J. H. Kim, S.-B. Cho, B. J. Kim, S. Yoon, B. J. Suh, S. W. Han, K. H. Kim, K. J. Kim, B. S. Kim, H. J. Song, H. J. Shin, J. H. Shim, and B. I. Min, *Appl. Phys. Lett.* **84**, 4233 (2004).

¹⁹S. Hüfner, *Photoelectron Spectroscopy*, Solid-State Sciences Vol. 82 (Springer-Verlag, Berlin, 1995).

²⁰J.-S. Kang, J. H. Kwak, Y. J. Shin, S. W. Han, K. H. Kim, and B. I. Min, *Phys. Rev. B* **61**, 10682 (2000).

²¹T. J. Regan, H. Ohldag, C. Stamm, F. Nolting, J. Lüning, J. Stöhr, and R. L. White, *Phys. Rev. B* **64**, 214422 (2001).

²²W. B. Wu, D. J. Huang, J. Okamoto, A. Tanaka, H.-J. Lin, F. C. Chou, A. Fujimori, and C. T. Chen, *Phys. Rev. Lett.* **94**, 146402 (2005).

²³C. T. Chen, Y. U. Idzerda, H.-J. Lin, N. V. Smith, G. Meigs, E. Chaban, G. H. Ho, E. Pellegrin, and F. Sette, *Phys. Rev. Lett.* **75**, 152 (1995).

²⁴I. Terasaki, Y. Sasago, and K. Uchinokura, *Phys. Rev. B* **56**, R12685 (1997).

²⁵K. Takada, H. Sakurai, E. Takayama-Muromachi, F. Izumi, R. A. Dilanian, and T. Sasaki, *Nature (London)* **422**, 53 (2003).

²⁶J.-S. Kang, S. W. Han, T. Fujii, I. Terasaki, S. S. Lee, G. Kim, C. G. Olson, H. G. Lee, J.-Y. Kim, and B. I. Min, *Phys. Rev. B* **74**, 205116 (2006).

²⁷T. Mizokawa, A. Fujimori, T. Arima, Y. Tokura, N. Mori, and J. Akimitsu, *Phys. Rev. B* **52**, 13865 (1995).

²⁸At 300 K, PrNiO_3 is in the metallic phase and expected to have a single phase of Ni^{3+} . See C. Piamonteze, F. M. F. de Groot, H. C. N. Tolentino, A. Y. Ramos, N. E. Massa, J. A. Alonso, and M. J. Martinez-Lope, *Phys. Rev. B* **71**, 020406(R) (2005).

²⁹M. A. van Veenendaal and G. A. Sawatzky, *Phys. Rev. B* **50**, 11326 (1994).

³⁰E. Wawrzyńska, R. Coldea, E. M. Wheeler, I. I. Mazin, M. D. Johannes, T. Sörgel, M. Jansen, R. M. Ibberson, and P. G. Radaelli, *Phys. Rev. Lett.* **99**, 157204 (2007).

³¹The magnetic structure of AF ordering in 3R-type AgNiO_2 has not been resolved yet.